Research

Ecography 38: 001–010, 2015
doi: 10.1111/ecog.01393

Subject Editor: Regan Early. Editor-in-Chief: Miguel Araújo. Accepted 1 May 2015

Evaluating methods to quantify spatial variation in the velocity of biological invasions

Clément Tisseuil, Aiko Gryspeirt, Renaud Lancelot, Maryline Pioz, Andrew Liebhold and Marius Gilbert

C. Tisseuil, A. Gryspeirt and M. Gilbert (marius.gilbert@ulb.ac.be), Biological Control and Spatial Ecology, Univ. Libre de Bruxelles, av FD Roosevelt 50, BE-1050 Brussels, Belgium. MG also at: Fonds National de la Recherche Scientifique, rue d'Egmont 5, BE-1000 Brussels, Belgium. – R. Lancelot, CIRAD, UMR CMAEE, Campus International de Baillarguet, BP, FR-34398 Montpellier, France, and INRA, UMR 1309, Campus International de Baillarguet, BP, FR-34398 Montpellier, France. – M. Pioz, INRA, UR 406 Abeilles et Environnement, Laboratoire Biologie et Protection de l'abeille, Site Agroparc, FR-84914 Avignon, France. – A. Liebhold, USDA Forest Service Northern Research Station, Morgantown, WV 26505, USA.

Invading species rarely spread homogeneously through a landscape and invasion patterns typically display irregular frontal boundaries as the invasion progresses through space. Those irregular patterns are generally produced by local environmental factors that may slow or accelerate movement of the frontal boundary. While there is an abundant literature on species distribution modelling methods that quantify local suitability for species establishment, comparatively few studies have examined methods for measuring the local velocity of invasions that can then be statistically analysed in relation to spatially variable environmental factors. Previous studies have used simulations to compare different methods for estimating the overall rate of spread of an invasion. We adopted a similar approach of simulating invasions that resemble two real case-studies, both in terms of their spatial resolution (i.e. considering the size of one cell as one km) and their spatial extent ($>600\,000$ km²). Simulations were sampled to compare how different methods used to measure local spread rate, namely the neighbouring, nearest distance and Delaunay methods, perform for spatio-temporal comparisons. We varied the assessment using three levels of complexity of the spatio-temporal pattern of invasion, three sample sizes (500, 1000 and 2000 points), three different spatial sampling patterns (stratified, random, aggregated), three interpolation methods (generalized linear model, kriging, thin plate spline regression) and two spatio-temporal modelling structures (trend surface analysis and boundary displacement), resulting in a total of 486 different scenarios. The thin plate spline regression interpolation method, in combination with trend surface analysis, was found to provide the most robust local spread rate quantification as it was able to reliably accommodate different sampling conditions and invasion patterns. This best approach was successfully applied to two case-studies, the invasion of France by the horse-chestnut leafminer *Cameraria ohridella* and by the bluetongue virus, generally in agreement with previously published values of spread rates. Potential avenues for further research are discussed.

The spread of invading organisms has historically attracted considerable attention. Interest has often focused on characterizing geographical patterns of spread, and with it, the speed of invasion (Hengeveld 1989, Bosch et al. 1992). One of the first mechanistic (mathematical) models describing invasion spread was proposed by Skellam (1951); this reaction-diffusion model coupled exponential growth with diffusive movement of invader populations. Several subsequent mathematical formulations built upon this model by accounting for elements such as a limited carrying capacity, different dispersal kernels (e.g. fat-tailed dispersal kernels; Kot et al. 1996), modes of dispersion (e.g. stratified dispersal; Shigesada and Kawasaki 1997), or the incorporation of density-dependent processes (e.g. Allee effect; Lewis and Kareiva 1993). In epidemiology, mechanistic models have a long history, with spatial models accounting for spatial contagion between populations of susceptible hosts and vectors through the use of transmission kernels (Keeling et al. 2001).

In both ecology and epidemiology, the use of mechanistic models generally requires a detailed understanding of key life-history parameters. Some of these can be inferred from historical invasions or epidemics through inverse modelling in which ranges of parameter values are tested to identify values that optimize the fit of the model to the observed data. But when the number of parameters increases, the volume of parameter space to be explored becomes high and the search for optimal combinations of parameters is thus computationally intensive. In contrast, empirical statistical models characterize the spatio-temporal patterns of invasions in order to quantify some of their key features (e.g. rate of spread, correlation between date of first invasion and external

predictor variables). These models are generally more difficult to interpret in biological or epidemiological terms, but have the comparative advantage of being much easier to fit to observed spatio-temporal data describing the invasion. The debate over the relative merits of process-based *vs.* empirical models has been on-going for a long time in ecology, in particular in the context of species distribution models (SDM; Kearney and Porter 2009, Buckley et al. 2010, Dormann et al. 2012). The careful application of empirical statistical modelling to quickly characterize an invasion pattern followed by the use of process-based models to test and validate more explicit hypotheses often represents a pragmatic and efficient approach (Dormann et al. 2012).

Quantifying the local spread of species from empirical data can provide valuable information about specific invasion systems. For example, estimates of local spread rate may be useful in species distribution modelling by providing inputs to hybrid models (Dormann et al. 2012) or to identify how environmental factors may influence the range expansion of a species. However, surprisingly few studies, either in ecology and epidemiology, have focused on the comparison of spread rate estimation methods. Of the few comparison studies, most have focused on the estimation of the general rate of spread i.e. the average rate of spread of an invasion over its entire duration and range (Gilbert and Liebhold 2010), rather than the velocity of the invasion at different locations within the invaded spatial domain.

However several studies have quantified local rates of spread using two general types of spatio-temporal analysis approaches. First, boundary displacement (BD) methods are based on the division of the invasion into discrete time steps and the offset of the invasion front between time steps is compared. The local spread rate is then estimated as the distance separating the invasion boundary between two successive time steps (Sharov and Liebhold 1998, Morin et al. 2009). By contrast, trend-surface analysis (TSA) uses the date of initial establishment as dependent variable at a set of locations and fits a spatial interpolation model to predict that date across the spatial domain as a function of spatial coordinates. The slope of the fitted surface can then be considered as a friction (units of time space^{-1}), and the local spread rate estimate can be calculated as the inverse of the friction (Farnsworth and Ward 2009, Pioz et al. 2011). These approaches have largely been developed independently, with implementation varying among specific studies where they were applied. For example, the TSA implementation of Farnsworth and Ward (2009) differed from that of Pioz et al. (2011) or of Firestone et al. (2011) by the method used to interpolate the date of first establishment. Several questions arise about these spread rate approaches. How should the observations be interpolated? How should one estimate the local spread rate once the spatio-temporal distribution of invaded areas is quantified? In addition, other questions arise about how best to sample invasion spread, including selection of sample density and spatial distribution of sampling.

Recently, several studies have compared the performance of various species distribution modelling methods based upon simulated data sets where predictor variables influencing the species occurrence are known a priori. Outputs from the different models are compared in their capacity to identify the effect of predictor variables (Dormann et al. 2007). In this paper, we adopted a similar strategy to investigate how various methods compare in their ability to quantify known local spread rates and evaluate their applicability to real case-studies. We first simulate the pattern of spread of a hypothetical invasive species according to a specific distribution of local spread, using a model similar to that used by Gilbert and Liebhold (2010). We then sampled simulation output as input to test various implementations of the BD and TSA approach and compared their outputs in term of accuracy and precision. In order to provide a more comprehensive data representation, we evaluated the various methods according to different sampling designs and levels of complexity in the simulated invasion process. The best performing method was applied to two real case-studies, the invasion of France by the horse-chestnut leafminer *Cameraria ohridella* and by the bluetongue virus.

Methods

Our analyses involved a series of five sequential steps, illustrated in Fig. 1, which were applied both to synthetic simulated data as well as to data from two case-studies of historical invasions. The first step involved simulating the invasion of an organism in a heterogeneous environment

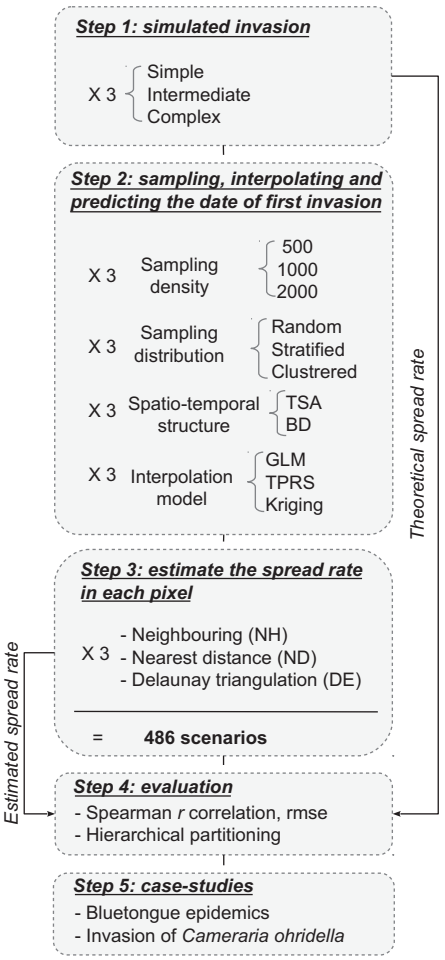

Figure 1. Summary of methods employed to evaluate different spread rate estimators.

consisting of a surface of random but autocorrelated growth rates (r). The simulations were designed to share patterns of invasions similar to those of the two real case-studies, both in terms of spatial resolution and in terms of spatial extent. The second step involved the sampling of the simulated spatio-temporal invasion data and use of these data to estimate the spatio-temporal distribution of the invasion front using different interpolation methods. The third step involved quantifying the local spread rate based on three estimators. The fourth step involved comparing the methods in their ability to estimate true spread rates under varying conditions (different sampling plans, interpolation methods, invasion patterns). The fifth step illustrates the application of the modelling framework to the two case-study applications. Each of these steps is detailed below.

Step one: simulated invasions

We used a simple coupled map lattice simulation model, described in Gilbert and Liebhold (2010). The advantage of this approach over similar models (Merow et al. 2011, Engler et al. 2012, Nobis and Normand 2014), was that the local expected theoretical spread rate could be directly calculated. This enabled us to assess the performance of various estimation methods (presented hereafter) to match the local theoretical spread rates.

The model is based on a deterministic formulation of Fisher's model (Fisher 1937), and includes two parts: 1) a discrete logistic population growth model (Eq. 1), and 2) a dispersal component assuming diffusion with a Gaussian dispersal kernel (Eq. 2). The model is discrete in time and space and operates over a matrix of 1000 by 1000 cells, as :

$$N'_{j,t+1} = N_{j,t} e^{r\left(1-N_{j,t}/K_i\right)} \quad (1)$$

$$N_{i,t+1} = \sum_{j=1}^{n} N'_{j,t+1} \times \frac{e^{\frac{-d_{i,j}^2}{4D}}}{4\pi D} \quad (2)$$

Where N_t and N_{t+1} are population sizes at time t and $t + 1$, D is the diffusion coefficient, K is the carrying capacity, $d_{i,j}$ is the distance between the point i and j, and r_i is the growth rate at cell i. The model was run along 240 times steps, but for the purpose of the analysis the simulations outputs were saved every 10 time-steps, resulting in the recording of 24 time-steps in the invasion process.

Three simulations of varying levels of spatial complexity in the spatio-temporal pattern of invasion were performed; they were designed to mimic realistic invasion patterns (Fig. 2) similar to those from the two case-studies described below. The focus of the model was not to fit the specific parameters of a particular invasion, but rather to produce invasions with varying degrees of spatial complexity in invasion pattern, based on varying theoretical local spread rates. Parameters having little influence on the spatio-temporal pattern of invasion (e.g. initial population, carrying capacity, diffusion coefficient) were hence kept constant. The simulation model parameter values (i.e. the variogram parameters defining the spatial autocorrelation structure in the growth parameter, r, the time and location of the initial colonization, general population model parameters) are reported in Table 1. In the 'simple' invasion scenario, the population was founded at a single, central point and the spatial autocorrelation of r was set to produce a relatively homogeneous spread pattern. The second simulation, referred to as the 'intermediate' scenario, was similar to the simple invasion, except that r exhibited a strong spatial autocorrelation structure, resulting from the combination of nested variogram models (Issaks and Srivistava 1990) with range parameters set empirically to 100 cells and 300 cells, respectively. The 'complex' invasion scenario used the same spatial autocorrelation structure as the 'intermediate' invasion scenario, but three different populations were introduced at different times and different locations. Multiple realisations of simulations were tested for each set of parameter values. They produced similar results and are not reported here.

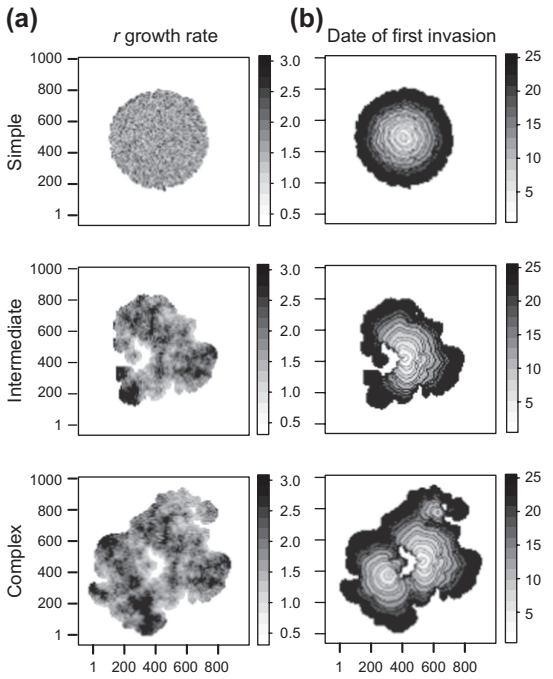

Figure 2. Illustration of the three patterns of invasion, ranging from simple to intermediate and complex. Each pattern was generated by varying the spatial contagion of the growth parameter, r, (a), and controlling the location(s) where founding populations were initialized (one location in the simple and intermediate pattern and three locations in the complex pattern). Simulations thus initialized generated markedly different patterns of the date of first invasion (b).

The theoretical rate of invasion spread (i.e. number of cells per unit time) produced by the Fisher model is approximated by Shigesada and Kawasaki (1997):

$$SR_{theo} = 2\sqrt{rD} \quad (3)$$

where r is the growth rate and D is the diffusion coefficient. This equation was used to estimate the theoretical ('true') invasion spread rate in each cell. Although most ecological invasions are known to result from both local and long-distance dispersal processes, it should be noted that the Fisher theoretical spread rate estimate used here only accounts for local dispersal processes. It is generally not possible to

Table 1. Simulations parameters.

	Simple	Intermediate		Complex	
Population models					
Number of individuals at start (N_0)	1000	1000		1000	
Carrying capacity (K)	1000	1000		1000	
Diffusion (D)	1	1		1	
Location and time initial colonization					
x (cell)	544	544	544	632	252
y (cell)	544	544	544	354	650
Time step (t/240)	1	1	1	40	80
Variogram parameters used to generate spatial autocorrelation structures in r growing parameter					
(Partial) sill	1	1		1	
Model type	Spherical	Spherical		Spherical	
Range (cell)	10	100–300		100–300	
Nugget component	0	0		0	

derive a theoretical constant spread rate from models that incorporate stochastic long-distance dispersal. Without such theoretical 'true' spread rates, cross-comparison with different spread rate estimation methods would not be possible and therefore we limited our study to the estimation of local spread rates driven by local dispersal.

Step two: sampling, interpolating and predicting the date of first invasion

We used three levels of sampling density ('low' for n = 500; 'medium' for n = 1000; and 'high' for n = 2000 sampling sites), in combination with three spatial patterns of sampling spatial distribution: 1) 'stratified', where one single random location was selected within the n windows splitting the geographical space; 2) 'random', for completely random spatial sampling, and 3), 'clustered', combining both random sampling and spatial sampling around 20 focal points (Supplementary material Appendix 1, Fig. A1). Those sampling schemes were designed to mimic hypothetical, but realistic, surveillance programs such as in the case-study of *Cameraria ohridella* (n = 1470). In the case-study of bluetongue epidemics, the number of observation locations was exceptionally high (n = 12 620), which provided a remarkably detailed spatio-temporal description of epidemic spread.

Each set of samples from each simulation was analysed using the BD and TSA methods. The BD method requires spatial interpolation of presence/absence from data sampled at each time step, whereas TSA uses a single spatial interpolation of the date of first invasion observed at each sample point. The typical output of the BD method is thus a temporal sequence of n presence/absence distribution maps coded as 1 and 0. These can be pooled into a single map by summing values from the sequence of presence/absence layers, with the value of each pixel representing the number of time steps for which the pixels was part of the invaded area. The typical output of the TSA interpolation is a map where each pixel value represents the time when it was first invaded. By taking n minus the pooled output map of the BD methods, where n is the total number of time steps, the output of the BD method becomes analogous to the TSA output, i.e. each pixel contains the time when it was first invaded. It is noteworthy that the output of the TSA is continuous whereas the output of the BD method is discrete.

Three interpolation methods were applied to each type of analysis of each set of samples of each set of simulated data. Several previous studies utilizing TSA conducted spatial interpolation using a generalized linear model (GLM) that fits linear, quadratic, cubic, and higher order trend-surfaces to data (Moore 1999, Lucey et al. 2002, Maidana and Yang 2009, Pioz et al. 2011). For spatial interpolation as part of the BD method, the GLM predicts a binomial response at each time step, whereas for the TSA method, the dependent variable was assumed to follow a Gaussian distribution. The BD method produces a continuous surface of probability of presence at each time step, which was converted to a binary presence/absence outputs using a fixed threshold of 0.5. In addition to GLMs, two other interpolation techniques were implemented: universal local kriging (Firestone et al. 2011), referred hereafter as 'Kriging', and generalized additive models using thin plate regression splines (Wood 2003, Farnsworth and Ward 2009), referred hereafter as '*TPRS*'. The spatial structure used in the Kriging model was estimated by fitting an experimental variogram (using generalized least squares regression) to data located within a 300 cells radius. The smoothing parameter in the *TPRS* model was estimated from sample data using generalized cross-validation, following the general procedure implemented in the 'fields' R packages (Furrer et al. 2013).

Step three: estimate the spread rate in each pixel

Three spread rate estimators were implemented to measure the local rate of spread for each pixel on the map of first date of invasion (illustrated in Fig. 3). In the first method, 'neighbouring' (NB), the spread rate is simply estimated as the inverse of the local slope of the date of first invasion surface (Fig. 3a). However, since the BD method produces discrete first dates of invasion, smoothing is applied using a local inverse distance weighting interpolation with a radius of 25 cells. Although the TSA produces continuous outputs, we applied the same smoothing filter so as to ensure comparability of the BD and TSA outputs. In the second method, called 'nearest distance' (ND), the distance of each pixel to the nearest previous and subsequent invasion front (border of

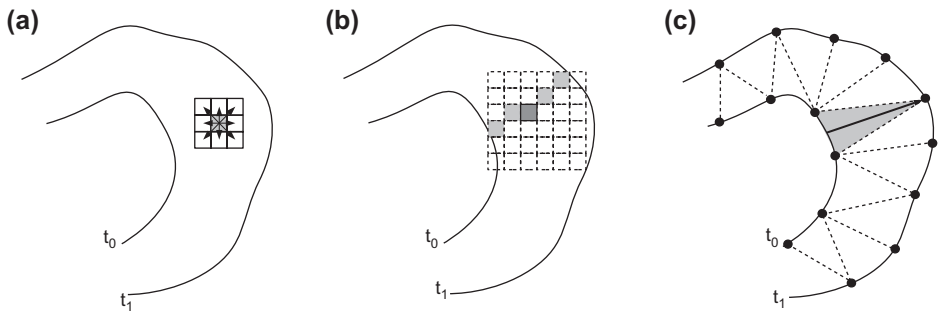

Figure 3. Illustration of the three spread rate estimators: (a) neighbouring; (b) nearest distance; (c) Delaunay.

presence and absence) was estimated and summed. The ND method can be thought as the length of the line that connects two sequential invasion front lines passing through a given pixel (Fig. 3b). Finally, in the third method, 'Delaunay' (DE), the space between two sequential invasion front lines was divided into geometric shapes using Delaunay triangulation (Fig. 4c). The triangles were built with two points located on the invasion front line at time t as the basis of the triangle, and connected to the nearest point of the next invasion front line at time $t + 1$. The length of the triangle median was used as a direct estimate of the local spread rate between two successive time steps.

Step four: evaluation

The overall validation step involved comparing the theoretical ('true') spread rates to the 486 estimated spread rates for each combination of the different varying factors in the analysis – i.e. the spread rate estimators (NB, ND or DE), the three types of invasion patterns (simple, intermediate, complex), the sampling density (low, medium, high), the sampling patterns (stratified, random, clustered), the spatio-temporal modelling structures (TSA or BD), and the interpolation methods (GLM, TPRS, Kriging). Theoretical and estimated spread rates were compared using two goodness-of-fit metrics, the Spearman r correlation coefficient (COR) and the root mean square error (RMSE), which assessed the precision and accuracy of predictions, respectively. Both metrics were replicated with a bootstrap procedure in which 1000 points were sampled randomly 10 times in the spatial domain (increasing the number of replicates up to 1000 did not notably impact the outputs results), both metrics calculated for each sample were then averaged over all bootstrap replicates.

The overall goodness-of-fit results were combined into a single database and hierarchical partitioning was used to quantify the relative influence of six distinct factors i.e. 1) spread rate estimators, 2) invasion pattern, 3) sampling density, 4) sampling pattern, 5) spatio-temporal modelling structure and 6) interpolation method, in explaining the variability of the two goodness-of-fit metrics (Chevan and Sutherland 1991). Hierarchical partitioning enables disentangling unique from joint effects among the different factors. It is thus possible to assess mutually non-exclusive interactions between factors. As long as the number of tested factors does not exceed nine, hierarchical partitioning provides reliable results (Olea et al. 2010).

Step five: case-studies

The optimal spread rate estimation method identified based upon simulations was applied to two case-studies to demonstrate the applicability of the method in different ecological systems: an epidemic of bluetongue virus (BT) and the invasion by the horse-chestnut leafminer *Cameraria ohridella,* both occurring in France during the 2000s. The aim was to demonstrate examples of how the spread rate analysis performs rather than to present a detailed analysis of each study-case. Both invasions shared spatial scales similar to those of the theoretical simulations, both in terms of spatial resolution (i.e. considering the size of one cell as one km) and spatial extent (>600 000 km²), which facilitated the

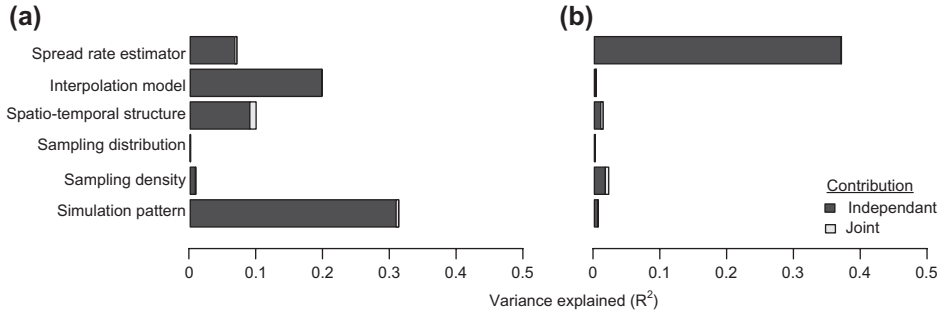

Figure 4. Hierarchical partitioning results showing the variance explained (adjusted R^2) by six factors (spread rate estimator, interpolation model, spatio-temporal modelling structure, sample spatial distribution, numbers of samples and pattern of invasion) on the two validation metrics: Spearman correlation (a) and the RMSE (b).

transferability of observations. Visually, the two case-studies exhibited patterns of invasions (Fig. 7) similar to the intermediate and complex theoretical scenarios generated by the simulation models (Fig. 2).

The first case-study was derived from Pioz et al. (2011), which analysed a bluetongue (BT) epidemic that occurred in France from July 2007 to December 2008. A case was defined as a bovine herd or an ovine or goat flock in which BT was clinically suspected and later confirmed by serological or virological analyses. The analysis was performed on a municipality basis (the smallest administrative unit in France) and cases with a missing date or location were discarded, leaving 33 042 cases in 12 620 municipalities. Spread analysis was based upon the first week of BT detection in each municipality. The spatial and temporal resolutions of the analyses were 1 km and 1 week, respectively.

The second case-study was taken from Gilbert et al. (2005) who analysed the invasion of the horse chestnut leafminer *Cameraria ohridella* (Lepidoptera, Gracillariidae) in France between 2000 and 2004. This leafminer is an invasive species first observed and identified in Macedonia in 1984, which has subsequently invaded much of central and western Europe over the following 30 yr at an approximate rate of 60 km yr^{-1}. In total, 5272 municipalities with presence/absence data were recorded, of which 1470 locations recording presence only were retained for the spread rate analysis on an annual basis.

Data available from the Dryad Digital Repository: <http://dx.doi.org/10.5061/dryad.c1d06> (Tisseuil et al. 2015).

Results

Sources of variability in RMSE and correlation results

On average, goodness-of-fit metrics yielded relatively low performance values with a high variability across the 486 scenarios (COR = 0.20 ± 0.22 SD; RMSE = 10.38 ± 1.87 SD). Hierarchical partitioning enabled disentanglement of the main sources of variability among the scenarios with slightly different results between the two metrics (Fig. 4). The correlation metric was predominantly affected by the invasion pattern ($R^2 = 0.32$), followed by the choice of interpolation method ($R^2 = 0.21$), and the spatio-temporal structure ($R^2 = 0.10$). In contrast, the RMSE metric was mainly affected by the spread rate estimator ($R^2 = 0.38$). For both metrics, sampling patterns and density accounted for a minor part of the variability ($R^2 < 0.05$).

Cross-relationships between RMSE and correlation results

Analysing the relationships between correlation and RMSE metrics across the 486 scenarios provided further insights into hierarchical partitioning results (Fig. 5; Supplementary material Appendix 1, Table A1). On average, the three spread rates estimators displayed concordant results, although better metric values were obtained with the NB than the DE and ND estimator (Fig. 5a). The dominant effect of interpolation method on spread rate correlation metrics was also revealed by the lowest performances of GLM methods, in comparison to TPRS and Kriging methods (Fig. 5b). With regard to the different invasion patterns, RMSE values were similar regardless of the pattern complexity, whereas the lowest correlation values were found for the simplest invasion pattern (Fig. 5c). Regarding the spatio-temporal modelling structure, TSA provided better goodness-of-fit than BD approaches (Fig. 5d). Increasing sampling density noticeably improved correlation and RMSE metric values (Fig. 5e), while the different sampling patterns did not result in substantial disparities in correlation and RMSE metrics (Fig 5f).

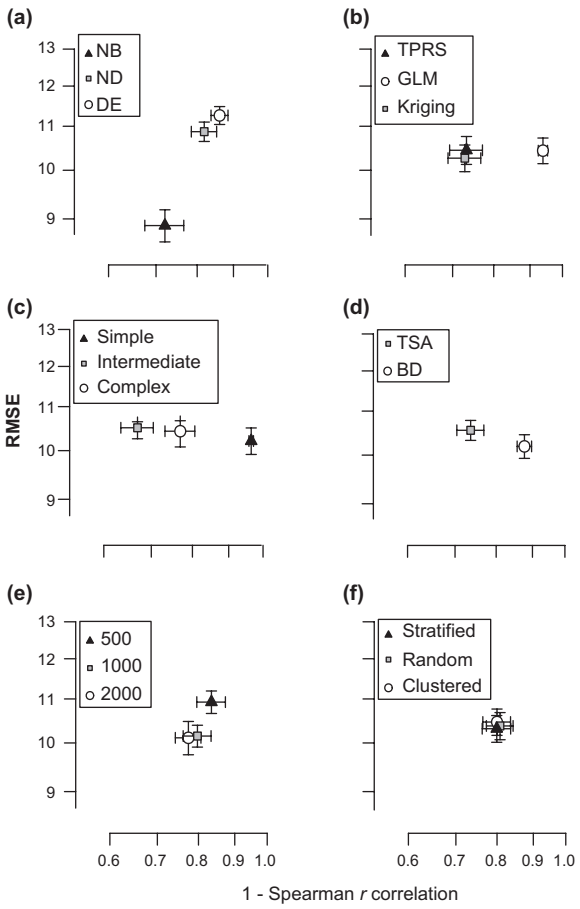

Figure 5. Relationships between averaged RMSE and Spearman correlation values with 95% confidence levels broken-down for the six tested factors: (a) spread rate estimator, (b) interpolation model, (c) pattern of invasion, (d) spatio-temporal modelling structure, (e) numbers of samples and, (f) the sample spatial distribution.

Optimal combination of methods to predict local spread rate

The optimal combination of spread rate estimator, spatio-temporal structure and interpolation method was selected as the one that maximized the correlation and minimized the root mean square error in the results (Fig. 6; bottom left area). The best results were obtained with the use of the NB spread rate estimator, in combination with a TSA spatio-temporal modelling structure and as spatial

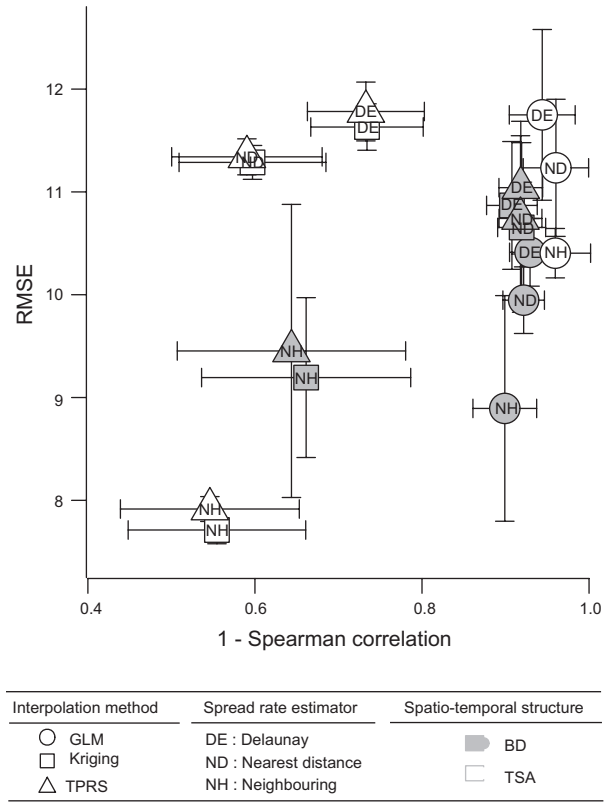

Figure 6. Characterization of the various approaches for estimating spread rate based on the relationships between the averaged RMSE and Spearman correlation values including 95% confidence levels. The 'boundary displacement' and 'trend surface analysis' spatio-temporal modelling structures are shown as white and grey, respectively. The three interpolation methods are symbolized by circles (GLM), squares (TPRS) and triangles (Kriging). The three spread rate estimators are identified as NB ('neighbouring'), ND ('nearest distance') and DE ('Delaunay').

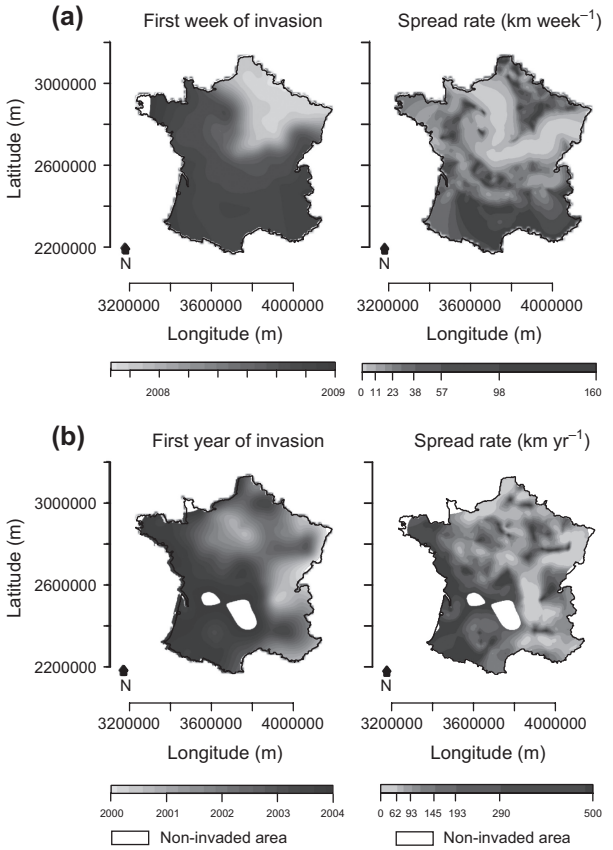

Figure 7. Analysis of historical spread across France from the two case-studies. The epidemic of bluetongue (BT) virus (a) and the invasion by *Cameraria ohridella* (b), using the best combination of spatio-temporal structure (i.e. TSA), interpolation method (i.e. TPRS) and spread rate estimates (i.e. NH).

interpolation method, either TPRS (COR = 0.45 ± 0.27 SD; RMSE = 7.92 ± 0.31 SD) or Kriging (COR = 0.44 ± 0.27 SD, RMSE = 7.71 ± 0.34 SD). Excluding GLM-based combination results, TSA results (in white) were more stable than BD results (in grey), in terms of reducing the variability in goodness-of-fit metrics among the different combinations of approaches. This conclusion was also reinforced by the pattern observed in Fig. 5d, showing that TSA results provided better goodness-of-fit metrics than BD results.

Case-studies

The optimal spread rate methods identified from the simulation studies (i.e. NH spread rate estimator based on TSA results using the TPSR interpolation method) were applied to the two case-studies (Fig. 7).

Application of the TSA method to the BT epidemics showed an overall north-east to south-west gradient of invasion. Although averaging 10 km week^{-1}, the spread rate of BT displayed high spatial heterogeneity (Fig. 7a). Local spread rate values were noticeably lower in the winter season presumably due to unfavorable environmental conditions constraining virus development, such as sub-optimal temperature or humidity.

From 2000 to 2004, *Cameraria ohridella* was gradually invading the western portion of France at an averaged speed of 63 km yr^{-1} (Fig. 7b). All areas with a year of first invasion extrapolated before 2000 or after 2004 were excluded from the spread rate calculation. Again, the local invasion spread rate displayed high heterogeneity in space that probably related to environmental heterogeneity in factors influencing dispersal or reproduction (e.g. weather, land cover, host density).

Discussion

Spread rate results from the simulation-based analysis are contrasted in terms of goodness-of-fit, as both the correlation and RMSE metrics displayed relatively weak and high variability across the 486 scenarios (COR = 0.20 ± 0.22 SD; RMSE = 10.38 ± 1.87 SD), and even the best scenarios provided relatively modest goodness-of-fit results (COR > 0.4; RMSE < 10). Six major issues should be addressed to

understand the relatively low performances and high variability in the results to draw meaningful conclusions.

First, the overall low performances values are based upon the reliability of the theoretical spread rate values, from which the estimated spread rate comparison is built upon. The theoretical spread rate is a mathematical approximation from the Fisher's model in a continuous space (Shigesada and Kawasaki 1997) and, to our knowledge, no theoretical study has investigated this in a spatially autocorrelated landscape. Therefore, what we consider as a 'theoretical' spread rate might in fact differ from what we could measure with a perfect method. This could explain some of the deviations observed between the estimated and theoretical spread rates, and support the idea that the goodness of fit metrics need to be interpreted and compared in relative rather than absolute terms.

Second, low correlation values should be interpreted with caution. The differences between the invasion patterns represent the major source of variability in the correlation values, mainly because the simple pattern of invasion resulted in the lowest correlation values on average. Concluding hastily that the spread rate methods have a weak ability to fit simple patterns of invasion would be misleading. Since a simple pattern of invasion is characterized by very homogeneous spread rates values in space, assessing spatial correspondence in such homogeneous space is difficult and tend to lead to poor correlation values. The analysis of spread rates results in simple invasion patterns should thus be considered using RMSE metrics only. In contrast, while complex patterns of invasion make them more difficult to predict, in terms of date of first invasion, their spread rate patterns are more structured in space than those from simple patterns. Therefore, correlation and RMSE values tend to increase as the pattern of invasion become more complex, which make the use of correlation metrics relevant for analysing sufficiently complex invasion patterns only. Filtering out the simplest pattern of invasion reveals that the more complex invasion pattern was sensibly more difficult to predict and generally resulted in lower goodness of fit metrics than the moderately complex invasion pattern. In conclusion, the comprehensive analysis of results suggests that the various spread rate methods have a relatively good ability to fit patterns of invasions of varying complexity.

Third, the method used to interpolate presence/absence data or the date of first invasion (GLM vs Kriging vs TPRS) was shown to be a secondary source of variability in the correlation metric, mainly due to GLM-based combinations of scenarios that tended to reduce the overall goodness-of-fit metrics. Even when incorporating high-order polynomial terms and spatial auto-correlation, GLM models are generally not effective interpolation methods and our results confirm that a much better fit can be obtained with TPRS and Kriging, with slightly better results for the TPRS method. However, the implementation of both methods involved unsupervised model fitting procedures. For Kriging, the semi-variogram model can strongly influence the quality of the interpolation, and better outputs could possibly be obtained through more supervised models i.e. based on knowledge of underlying ecological processes, to ensure that the semi-variance model adequately fits the experimental semi-variogram (Issaks and Srivistava 1990). However, for the same reason, TPRS may represent a desirable alternative as it requires relatively little experience in spatial modelling and a priori little knowledge of the underlying ecological processes. Our results suggest that TPSR had a slightly better goodness of fit and was approximately 20 times faster than Kriging. This may become a particularly important practical issue for studies covering wide spatial extents with high spatial resolution. As a recommendation, the user may wish to base their selection of spatial interpolation methods based upon practical matters.

Fourth, the main source of variability in RMSE values was related to the differences between the three spread rate estimators (ND, NB and DE). It is noteworthy that the choice of spread rate method is closely linked to that of the previous modelling options. For example, the DE and ND methods are more appropriate to the BD spatio-temporal modelling structure that provides a presence/absence boundary line at each time step (i.e. discrete modelled time of invasion), because they will each quantify the distance between two isolines. Similarly, the NB method is more appropriately applied to the outputs of TSA that predict the time of invasion on a continuous scale. Because the combination of TSA and TPRS had the best goodness of fit metrics, the most suited spread rate estimator appears to be the NB, which also showed the highest goodness of fit metrics. However, the NB method has some unique problematic features that would need to be filtered out. For example, if adjoining pixels have identical estimated times of invasion, the local slope is null, and the rate of spread, which is estimated as the inverse of the slope becomes locally infinite. These artefacts can be reduced by increasing the size of the windows used to estimate the slope, but this is done at the expense of loosing spatial detail. Application of this method also requires that uninvaded areas must be removed from the spatial domain of the analysis, which could be done, for instance, by modelling first the spatial distribution of invasion prior and then deriving the spread rate estimates to the restricted invaded area.

Five, the spatio-temporal structure (i.e. BD vs TSA) accounted for less than 10% of the variability in the goodness-of-fit metrics, indicating that the selection of one approach had less influence on local spread rate estimates than previously expected. Surprisingly, the TSA approach displayed noticeably better goodness-of-fit results than the BD approach which was anticipated to provide a more detailed analysis of spread at each time step of the invasion. Furthermore, because of the need to interpolate the presence/absence distribution at each time step, the BD method requires much more processing time than the TSA approach. Thus, TSA combined with interpolation of the time of establishment using TPRS appears as the best combination of methods both from accuracy and processing time perspectives.

Finally, the numbers of sampling points and spatial pattern of samples also had a comparatively low impact on spread estimates, although results from higher sampling density displayed slightly better goodness-of-fit metrics than those with a lower density. This may have resulted from the limited range of sampling procedures that was tested (i.e. one would have degraded estimates with very low sampling densities). Perhaps more surprising was the relatively minor influence of the spatial pattern of the sampling points. It is

likely that the influence of sample arrangement was effectively masked by the variability due to the different interpolation methods. Here too, more extreme sampling conditions with very high level of clustering would probably have resulted in a stronger effect, but such patterns would probably not be realistic since actual design of sampling would presumably attempt to avoid such extreme configurations.

From this set of analyses, and within the range of invasion patterns that were tested, our results highlighted the combination of TSA and TPRS, followed by a local estimator of slope, the NB method (TSA-TPRS-NB), as a preferred approach, both in terms of goodness of fit and processing time. The method was robust to complex patterns of invasions, aggregated sampling distribution and low sample density.

The TSA-TPRS-NB approach was satisfactorily applied to the two case-studies, revealing results consistent with those in the literature, both in terms of global and local spread rate of invasions. Regarding *Cameraria ohridella*, Gilbert et al. (2005) reported global spread rate estimates averaging 60 km yr^{-1} while our analysis indicated a median speed of 63 km yr^{-1}. In a previous study, Augustin et al. (2004) analysed the local spread rate estimates of *Cameraria ohridella* in a northern region of France. Over the period 2001–2003, the spread rate ranged from 17.0 to 37.9 km yr^{-1}, depending on the population threshold and method used. Extracted over the same region, our local spread rates estimates yield similar results with a median of 36 km yr^{-1}. Regarding the BT case-study, our results draws similar conclusions than Pioz et al. (2011, 2012). The authors used trend surface analysis with an interpolation of the date of first invasion in French municipalities based on a simultaneous autoregressive (SAR) model followed by a local estimate of the slope obtained through derivation, that would be closest to our TSA-GLM-NB implementation. The authors estimated the mean velocity of the front-wave of invasion between 2.1 and 9.3 km $week^{-1}$, which is sensibly lower than our spread rate estimations of approximately 10 km $week^{-1}$. Both case studies highlight the high spatial variability in spread rate estimates, emphasizing the potential role of environmental factors (e.g. climate, land cover, host density) in influencing local spread rate.

Our study is a solid baseline and provides new insights for future research. One important caveat is that our modelling approach relies on an assumption that simulated spread scenarios are comparable to real world invasion spread patterns. Although our two case-studies provide evidence of local-spread processes responsible for spatio-temporal patterns of invasion, we acknowledge that important sources of stochasticity, such as habitat heterogeneity or long-distance dispersal, may also play a determinant role. Incorporating such stochastic processes into our modelling framework would make it challenging to derive a theoretical spread rate to which estimated spread rates could be compared. Using the estimated spread rate to forecast spatio-temporal patterns of invasions into the future would be another fascinating subject for further research. Such work would require development of methods for quantifying uncertainty in estimated spread rates and incorporating that into forecasts. A potential avenue for future research would also be to delve further into how the parameters used in our simulations relate to the observed invasions, noting differences in numbers of initial populations, estimates for initial population sizes, mechanisms of spread, etc.

To conclude, this study is the first attempt, to our knowledge, to evaluate different methods for estimation of local spatial spread rates, while previous studies have compared methods for estimation of global rates of spread (Tobin et al. 2007, Gilbert and Liebhold 2010). Based upon our results, we recommend the use of any one of several spatial interpolation methods followed by the application of a local estimator of slope to derive estimates of local spread rate, which appears robust to varying patterns of invasions and sampling conditions. The method was successfully applied to the two case-studies yielding global spread rate estimates that were consistent with previous estimates from the literature. Further research could apply the set of methods tested here to other empirical data sets to shed light on their practical ease of implementation, conditions of use, and capacity to produce meaningful local spread rate estimates that could then be analyzed against factors influencing spread.

Acknowledgements – This study was funded by EU grant FP7-261504 EDENext and is catalogued by the EDENext Steering Committee as EDENext259 (<www.edenext.eu>). The contents of this publication are the sole responsibility of the authors and don't necessarily reflect the views of the European Commission.

References

Augustin, S. et al. 2004. Monitoring the regional spread of the invasive leafminer *Cameraria ohridella* (Lepidoptera: Gracillariidae) by damage assessment and pheromone trapping. – Environ. Entomol. 33: 1584–1592.

Bosch, F. van den et al. 1992. Analysing the velocity of animal range expansion. – J. Biogeogr. 19: 135–150.

Buckley, L. B. et al. 2010. Can mechanism inform species' distribution models? – Ecol. Lett. 13: 1041–1054.

Chevan, A. and Sutherland, M. 1991. Hierarchical partitioning. – Am. Stat. 45: 90–96.

Dormann, C. F. et al. 2007. Methods to account for spatial autocorrelation in the analysis of species distributional data: a review. – Ecography 30: 609–628.

Dormann, C. F. et al. 2012. Correlation and process in species distribution models: bridging a dichotomy. – J. Biogeogr. 39: 2119–2131.

Engler, R. et al. 2012. The MIGCLIM R package – seamless integration of dispersal constraints into projections of species distribution models. – Ecography 35: 872–878.

Farnsworth, M. L. and Ward, M. P. 2009. Identifying spatio-temporal patterns of transboundary disease spread: examples using avian influenza H5N1 outbreaks. – Vet. Res. 40: 20.

Firestone, S. M. et al. 2011. The importance of location in contact networks: describing early epidemic spread using spatial social network analysis. – Prev. Vet. Med. 102: 185–195.

Fisher, R. A. 1937. The wave of advance of advantageous genes. – Ann. Eugen. 7: 355–369.

Furrer, R. et al. 2013. Fields: tools for spatial data. – R package ver. 6.8.

Gilbert, M. and Liebhold, A. 2010. Comparing methods for measuring the rate of spread of invading populations. – Ecography 33: 809–817.

Gilbert, M. et al. 2005. Forecasting *Cameraria ohridella* invasion dynamics in recently invaded countries: from validation to prediction. – J. Appl. Ecol. 42: 805–813.

Hengeveld, R. 1989. Dynamics of biological invasions. – Springer.
Isaaks, E. H. and Srivastava, R. M. 1990. An introduction to applied geostatistics. – Oxford Univ. Press.
Kearney, M. and Porter, W. 2009. Mechanistic niche modelling: combining physiological and spatial data to predict species' ranges. – Ecol. Lett. 12: 334–350.
Keeling, M. J. et al. 2001. Dynamics of the 2001 UK Foot and Mouth epidemic: stochastic dispersal in a heterogeneous landscape. – Science 294: 813–817.
Kot, M. et al. 1996. Dispersal data and the spread of invading organisms. – Ecology 77: 2027–2042.
Lewis, M. A. and Kareiva, P. 1993. Allee dynamics and the spread of invading organisms. – Theor. Popul. Biol. 43: 141–158.
Lucey, B. T. et al. 2002. Spatiotemporal analysis of epizootic raccoon rabies propagation in Connecticut, 1991–1995. – Vector-Borne Zoonotic Dis. 2: 77–86.
Maidana, N. A. and Yang, H. M. 2009. Spatial spreading of West Nile Virus described by traveling waves. – J. Theor. Biol. 258: 403–417.
Merow, C. et al. 2011. Developing dynamic mechanistic species distribution models: predicting bird-mediated spread of invasive plants across northeastern North America. – Am. Nat. 178: 30–43.
Moore, D. A. 1999. Spatial diffusion of raccoon rabies in Pennsylvania, USA. – Prev. Vet. Med. 40: 19–32.
Morin, R. S. et al. 2009. Anisotropic spread of hemlock woolly adelgid in the eastern United States. – Biol. Invasions 11: 2341–2350.

Supplementary material (Appendix ECOG-01393 at <www.ecography.org/readers/appendix>). Appendix 1.

Nobis, M. P. and Normand, S. 2014. KISSMig – a simple model for R to account for limited migration in analyses of species distributions. – Ecography 37: 1282–1287.
Olea, P. P. et al. 2010. Estimating and modelling bias of the hierarchical partitioning public-domain software: implications in environmental management and conservation. – PLoS One 5: e11698.
Pioz, M. et al. 2011. Estimating front-wave velocity of infectious diseases: a simple, efficient method applied to bluetongue. – Vet. Res. 42: 60.
Pioz, M. et al. 2012. Why did Bluetongue spread the way it did? Environmental factors influencing the velocity of Bluetongue virus serotype 8 epizootic wave in France. – PLoS One 7: e43360.
Sharov, A. A. and Liebhold, A. M. 1998. Quantitative analysis of gypsy moth spread in the central Appalachians. – In: Baumgartner, J. et al. (eds), Population and community ecology for insect management and conservation. Balkema, pp. 99–110.
Shigesada, N. and Kawasaki, K. 1997. Biological invasions: theory and practice. – Oxford Univ. Press.
Skellam, J. G. 1951. Random dispersal in theoretical populations. – Biometrika 38: 196–218.
Tisseuil, C. et al 2015. Data from: Evaluating methods to quantify spatial variation in the velocity of biological invasions. – Dryad Digital Repository, <http://dx.doi.org/10.5061/dryad.c1d06>.
Tobin, P. C. et al. 2007. Comparison of methods for estimating the spread of a non-indigenous species. – J. Biogeogr. 34: 305–312.
Wood, S. N. 2003. Thin plate regression splines. – J. R. Stat. Soc. B 65: 95–114.